Angular momentum effects in heavy-ion-induced fission

A. D'Arrigo, G. Giardina, M. Herman, and A. Taccone
Dipartimento di Fisica dell'Universita' di Messina and Istituto Nazionale di Fisica Nucleare, Gruppo Collegato di Messina Salita Sperone 31, 98166 Vill S. Agata-Messina, Italy
(Received 3 April 1992)

We analyze angular momentum effects in heavy-ion-induced fission in terms of the statistical model, including collective effects in the nonadiabatic approach and avoiding all the usual numerical approximations and free parameters but one. We find that the strong increase of the fission probability along with the increasing compound nucleus spin is responsible for several observable effects such as the increase of the fission cross section and the decrease of the multiple-chance fission contribution, with the increase of the projectile mass. It is shown that the fission is particularly sensitive to the fusion cross section and its spin distribution. This feature can be used to determine the latter two from the measured fission cross section.

PACS number(s): 25.85.−w

I. INTRODUCTION

Nuclear fission has been an extensively studied field of nuclear physics for a long time. As far as a neutron-induced fission is concerned, one can assume that the process is rather well understood in terms of the statistical model and its cross section can be predicted with relatively high accuracy by existing model codes. Introduction of heavy-ion (HI) beams has brought about new qualities in this well-established field. Not only has the range of the nuclei of interest been vastly enlarged, but most of all formation of the very-high-spin states in HI reactions requires a more careful and accurate treatment of the angular momentum effects. One of the aims of this paper is to demonstrate the importance of these effects and to indicate how they can eventually be employed for the determination of the quantities, which, not being direct observables, are otherwise difficult to estimate.

It is known that the fission cross section strongly depends on the following spin-dependent quantities: (i) the compound-nucleus fusion cross section, (ii) level densities in the nucleon emission and fission channels, and (iii) the fission barrier. None of these quantities is, however, entirely available for experimental investigations. The fusion cross section can be determined experimentally by measuring cross sections in all exit channels, but its spin distribution remains a subject of theoretical speculation. Similarly, level densities can be studied experimentally only in a very limited range of low spins and energies, far from the values typical for HI reactions. The same also holds for the spin dependence of a fission barrier which usually relies on the liquid-drop-model predictions. To investigate the role of angular momentum, we extended the statistical model code EMPIRE [1], based on the Hauser-Feshbach theory, to include HI-induced fission. In doing this we were guided by the work of Vigdor and Karwowski [2], especially in the parts related to nuclear deformation effects. We avoid, however, certain numerical approximations and extend our investigations to the very-high-spin values approaching the limits of nuclear stability. Under such extreme conditions, we had to pay appropriate attention to effects related to nuclear shapes which undergo a dynamical evolution with increasing spin. We account for the accurate angular momentum and parity coupling and allow for a fission preceded by a multiparticle emission.

We consider ^{158}Er, for which fission cross sections had been measured for various incoming channels and energies by van der Plicht *et al.* [3]. Having the same compound nucleus formed in different incoming channels is much to our advantage because of the following: (i) it offers the possibility of forming the same compound nucleus (CN) at the same excitation energy, but with a very different spin population (exhibiting the role played by the angular momentum); (ii) all CN and residual nuclei-related quantities have to be kept the same for each projectile-target combination, providing a more severe test of the model itself.

II. MODEL

In the frame of statistical theory, the contribution of the CN state with spin J, parity π, and excitation energy E to the fission cross section is given by the ratio of the fission width Γ_f to the total width $\Gamma_{\rm tot}$ multiplied by the population of this state, $\sigma(E,J,\pi)$. This general approach holds not only for the first CN following HI absorption, but also for the secondary CN's which are formed as a result of subsequent emission of particles. The only difference is that while the first CN is excited to the unique (incident channel compatible) energy, the secondary CN's are created with excitation energies which spread over an available interval. Each of the CN states contributes to the fission cross section with

$$\sigma_f(E,J,\pi)=\sigma(E,J,\pi)\frac{\Gamma_f(E,J,\pi)}{\sum_x \Gamma_x(E,J,\pi)} , \quad (1)$$

which has to be summed up over spin and parity, integrated over excitation energy, and finally summed over all the nuclei in the decay chain to obtain the measured fission cross section. The fission and particle decay widths are given by the formulas

$$\Gamma_f(E,J,\pi)=\frac{1}{2\pi\rho_{\rm CN}(E,J,\pi)}\int_0^{E-E_{\rm sad}(J)}\rho_f(E-E_{\rm sad}(J)-\epsilon,J,\pi)T_f(E-\epsilon)d\epsilon\ , \tag{2}$$

$$\Gamma_x(E,J,\pi)=\frac{1}{2\pi\rho_{\rm CN}(E,J,\pi)}\sum_{J'=0}^{\infty}\sum_{\pi'}\sum_{j=|J'-J|}^{J+J'}\int_0^{E-B_x}\rho_x(E-B_x-\epsilon,J',\pi')T_x^{l,j}(\epsilon)d\epsilon\ , \tag{3}$$

where $E_{\rm sad}(J)$ is the energy of the nucleus at the saddle point with angular momentum J, ρ is the level density, and T stands for the transmission coefficient. The subscripts f and x refer, respectively, to the fission process and particle-x emission channels (neutron, proton, α, and γ). The subscript CN indicates compound nucleus, and primes are used to mark a residual nucleus after particle emission. The parity selection rules are implicit in Eq. (3).

$T_x^{l,j}$ is an optical-model transmission coefficient for particle x with orbital angular momentum l coupled with particle spin to give j. The fission transmission coefficient T_f is taken in the classical form proposed by Hill and Wheeler [4]:

$$T_f=[1+\exp(-2\pi E/\hbar\omega)]^{-1}\ , \tag{4}$$

with $\hbar\omega=1$ MeV. In the present cases, the fission transmission coefficient is practically equal to unity, as a result of the rather high excitation energies involved, and therefore the particular choice of the $\hbar\omega$ value is irrelevant.

To estimate the fusion cross section, we apply the Bass model [5], which is supposed to provide the total fusion cross sections with accuracy of the order of 10%. This cross section is distributed among different spins of compound nucleus by means of the l-wave transmission coefficients

$$T_l=\left[1+\exp\frac{l-l_{\rm fus}}{d}\right]^{-1}\ . \tag{5}$$

Here d is a free parameter and $l_{\rm fus}$ is chosen in such a way that, having d fixed, $\sum_l(2l+1)T_l$ equals the cross section of Bass. Such an approach is based on the assumption that a transmission coefficient for HI fusion equals unity for l's lower than $l_{\rm fus}$ and falls off smoothly to zero for greater l's. It follows that the fusion cross section reaches its maximum at J somewhat lower than $l_{\rm fus}$. Calculating spin distribution, we couple projectile spin and orbital momentum with the target spin to the compound-nucleus state spin J, observing parity conservation.

Special attention has been devoted to the treatment of the level densities. HI-induced fission involves very high spins which inhibit the usual factorization of the spin-dependent part in the level-density formula. In addition, large nuclear deformations bring about a rotational enhancement of the level densities. This enhancement is especially effective in the fission channel, but also persists in the particle channels because of the dynamic deformation of the high-spin states. To account for rotational enhancement and to avoid a spin factorization assumption, we apply the expressions reported in Ref. [6] [Eqs. (4-63b) and (2B-51)] and write the density of levels with spin J at energy E as

$$\rho(E,J,\pi)=\frac{1}{16\sqrt{6\pi}}\left[\frac{\hbar^2}{\mathcal{I}_\parallel}\right]^{1/2}a^{1/4}\sum_{K=-J}^{J}[E-E_{\rm rot}(K)]^{-5/4}\exp(2\{a[E-E_{\rm rot}(K)]\}^{1/2})\ ,$$
$$E_{\rm rot}(K)=\frac{\hbar^2}{2\mathcal{I}_\perp}J(J+1)+\frac{\hbar^2K^2}{2}\left[\frac{1}{\mathcal{I}_\parallel}-\frac{1}{\mathcal{I}_\perp}\right]\ . \tag{6}$$

Here $\mathcal{I}_\perp$ and $\mathcal{I}_\parallel$ are moments of inertia perpendicular and parallel to the symmetry axis and K is the projection of J on the quantization axis. Application of this general expression depends on the particular case. A nucleus at the saddle point is known to have a strong prolate deformation with the angular momentum vector perpendicular to the symmetry axis and therefore the rotational contribution to $E_{\rm sad}(J)$ is given by

$$\hbar^2J(J+1)/2(\mathcal{I}_\perp)_{\rm sad}\ . \tag{7}$$

In the case of the yrast state (equilibrium state of the residual nucleus reached after particle or gamma emission), the deformation is usually slight and the shape may be prolate, oblate, or even triaxial. For prolate yrast deformations, we assume rotation around the axis perpendicular to the symmetry axis and retain expression (7) to calculate the rotational-energy contribution. In the case of the oblate deformation, however, the nucleus is assumed to rotate around its symmetry axis and the rotational energy contribution to the potential-energy surface becomes

$$\hbar^2J(J+1)/2(\mathcal{I}_\perp)_{\rm yr}\ . \tag{8}$$

Defining the effective moment of inertia,

$$\frac{1}{\mathcal{I}_{\rm eff}}=\frac{1}{\mathcal{I}_\parallel}-\frac{1}{\mathcal{I}_\perp}\ , \tag{9}$$

the level densities for prolate and oblate deformed nuclei read

$$\rho(E,J,\pi)=\frac{1}{16\sqrt{6\pi}}\left[\frac{\hbar^2}{\mathcal{I}_\parallel}\right]^{1/2}a^{1/4}\sum_{K=-J}^{J}\left[U-\frac{\hbar^2K^2}{2\mathcal{I}_{\rm eff}}\right]^{-5/4}\exp\left\{2\left[a\left[U-\frac{\hbar^2K^2}{2\mathcal{I}_{\rm eff}}\right]\right]^{1/2}\right\} \tag{10}$$

and

$$\rho(E,J,\pi)=\frac{1}{16\sqrt{6\pi}}\left[\frac{\hbar^2}{\mathcal{I}_\parallel}\right]^{1/2}a^{1/4}\sum_{K=-J}^{J}\left[U-\frac{\hbar^2[J(J+1)-K^2]}{2|\mathcal{I}_{\rm eff}|}\right]^{-5/4}\exp\left\{2\left[a\left[U-\frac{\hbar^2[J(J+1)-K^2]}{2|\mathcal{I}_{\rm eff}|}\right]\right]^{1/2}\right\}. \tag{11}$$

Note that for the density of fission channels Eq. (10) is appropriate, while either of the two expressions [Eqs. (10) and (11)] can be valid for the yrast states, depending on their deformation. Consistency requires that for the critical value of the angular momentum—for which the fission barrier vanishes—saddle-point and yrast shapes are the same and level densities are calculated using the same analytical form.

Equations (6), (10), and (11) describe an adiabatic limit in which intrinsic and rotational degrees of freedom are completely decoupled. In fact, a rotational band is built on each intrinsic state, which leads to an increase of the total level density by factor of the order of 10^2. This assumption ceases to be valid for higher excitation energies. Indeed, the cranking-model Hamiltonian contains the Coriolis term, which directly couples intrinsic and rotational motions and eventually leads to the breakdown of the adiabatic approach. One expects the relevant scale to be given by the Coriolis energy [2,6], which may be approximated as

$$E_{\rm cor}({\rm MeV})\simeq\hbar\omega_0|\delta_{\rm osc}|=41A^{-1/3}|\delta_{\rm osc}|\ , \tag{12}$$

where $\hbar\omega_0$ is the mean oscillator frequency and $\delta_{\rm osc}$ is the potential deformation parameter. Following [2], we account for the damping of the rotational enhancement multiplying Eqs. (10) and (11) by

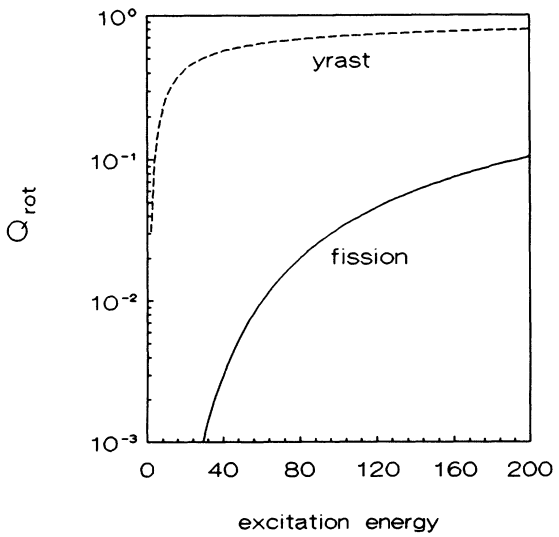

FIG. 1. Energy dependence of $Q_{\rm rot}$ used to damp the rotational enhancement of level densities for saddle point and yrast deformations.

$$1-Q_{\rm rot}\left[1-\frac{1}{\hbar^2/\mathcal{I}_\perp t}\right]. \tag{13}$$

This expression is tailored to approach unity, essentially leaving the entire rotational contribution to the level densities intact, at temperatures t low compared with $E_{\rm cor}$, and tends to the inverse of the rotational enhancement factor $\hbar^2/\mathcal{I}_\perp t$ at $t\gg E_{\rm cor}$, leading to the cancellation of the rotational enhancement. To this end, the $Q_{\rm rot}$ function is arbitrarily related to the Fermi-gas occupation probability of the single-particle level at energy $E_{\rm cor}$:

$$Q_{\rm rot}=\frac{2}{\exp(E_{\rm cor}/t)+1}\ . \tag{14}$$

Figure 1 illustrates the energy dependence of $Q_{\rm rot}$ for the yrast and saddle-point cases. It should be stressed that because of the much larger deformation of the saddle point, rotational enhancement fadeout in the fission channel is considerably slower than in the particle emission channels. Later on, we shall return to discuss consequences of this difference.

In addition to the rotational effects, we also account for the vibrational enhancement of the level densities multiplying Eqs. (10) and (11) by the factor $K_{\rm vibr}-Q_{\rm vibr}(K_{\rm vibr}-1)$, where, following Ref. [7],

$$K_{\rm vibr}=\exp\left[1.7\left[\frac{3m_0A}{4\pi\hbar^2\sigma_{\rm drop}}\right]^{2/3}t^{4/3}\right] \tag{15}$$

and

$$Q_{\rm vibr}=\left[1+\exp\frac{t_{1/2}-t}{d_t}\right]^{-1}. \tag{16}$$

Here m_0 is the nucleon mass and $\sigma_{\rm drop}$ is the coefficient of the surface tension in the liquid-drop model. As for the rotational effects, one expects the vibrational enhancement to vanish at high temperatures. Equation (15) therefore contains a damping factor $Q_{\rm vibr}$, which we arbitrarily choose to be $\frac{1}{2}$ at $t=t_{1/2}=2$ MeV with $d_t=0.2$ MeV. In practice, this choice is of little importance because the vibrational enhancement affects fission and particle channels in a similar way and to a large extent it cancels in the fission cross-section formula. We have checked that by forcing the damping factor to reach a $\frac{1}{2}$ value at $t=1$ MeV instead of 2 MeV, the fission cross section is practically unaltered.

III. CALCULATIONS

In our calculations we consider first-, second-, and third-chance fissions, allowing for the competition of neutron, proton, and α emission. In the case of second- and

third-chance fissions, we also account for the full γ cascade, which at lower energies may effectively compete with the particle and fission channels. For completeness, in addition to the decay to continuum, we also include particle and γ decay to the few low-lying resolved levels, even though their contributions turn out to be negligible. Throughout this paper we neglect the possibility of having multiple-chance fission after emission of any charged particle. This could be done with our code, but these processes contribute too little to justify a huge calculation effort.

It is important for all relevant parameters used in the calculations to be specified in detail since, in principle, our conclusions may depend on the choice of the input. In fact, the same result may be usually obtained with a different choice of input parameters and it is difficult to establish where the physics ends and the game starts. That is why we choose to study the same compound nucleus produced in different reactions, which needs a simultaneous reproduction of the enlarged body of experimental data nearly with the same set of parameters. The only parameter which is evidently related to the incoming channel is d, which describes deviations from the sharp cutoff in the spin distribution of the fusion cross section. This parameter was actually the only one fitted (to the low-energy fission cross sections) and will be discussed further on. All the remaining calculation ingredients were chosen on physical bases and kept fixed throughout the computations.

The transmission coefficients $T_x^{l,j}$ for the particle channels were calculated from a spherical optical-model potential with global parameters by Becchetti and Greenlees [8]. The use of the spherical optical model is to some extent inconsistent with the large deformations encountered in the calculations. The effect of the nuclear deformation on the transmission coefficients was studied in Ref. [2]. The main effect of the deformation was found to consist in the shift of the transmission coefficient thresholds toward lower energies. This shift is of the order of 1 MeV and may eventually lead to a substantial modification of the charged-particle emission close to the threshold, but should not be relevant for the fission cross section.

In order to determine the level-density parameter a, we applied the method proposed in Ref. [9] and calculated a from the single-particle spectrum of the shell-model Hamiltonian. We favor this method over the standard parametrization $a = A/c$ (with $c \simeq 8$), as it is not only realistic, but it also takes care of the energy and mass dependences resulting from the shell structure in the eigenvalue spectrum. For the time being, we neglect the difference between the single-particle spectrum at the ground state and saddle point. As a matter of fact, a large saddle-point deformation may lead to some increase of a and consequently to an increase of the fission cross section, but this effect is estimated to be rather small [10].

Other parameters of crucial importance are moments of inertia which determine the spin distribution of the levels. In the case of the saddle point, the three principal moments of inertia were obtained by means of Sierk's routine BARMOM [11], which fits the results of the advanced rotating liquid-drop-model (RLDM) calculations. The inertia moments for the yrast states were calculated from the β and γ deformation parameters using the formulas reported in the Appendix of Ref. [2]. The spin-dependent deformation parameters were taken from Ref. [12], in which the shape of different even isotopes of Er were studied in the frame of the cranking model. Out of these we chose ^{158}Er and applied its shape indifferently to all the nuclei involved. According to Ref. [12], ^{158}Er is prolate up to spins of about $40\hbar$ with $\beta = 0.2$–0.3, for higher spins it crosses the triaxial region to reach the axially symmetric oblate deformation at $J = 50\hbar$, and for further spin increase it remains oblate, increasing its β deformation parameter. This leads to an increase of the inertia moment, which must not be neglected when heavy projectiles and high incident energies are considered.

The spin-dependent fission barriers were obtained using the BARFIT routine [11] based on the same RLDM calculations, which also provided moments of inertia. The same routine, in addition, returns ground-state energy at a given spin, which is used to determine the effective excitation energy in the fission and particle emission channels.

The remaining model parameters (ejectiles' binding energies and fusion Q value) were calculated from the tables of nuclear masses [13], and all spins were taken from [14].

IV. ANGULAR MOMENTUM EFFECTS

The results of our theoretical calculations are compared with experimental data in Fig. 2. We believe the general agreement to be more than satisfactory. Some minor deviations could easily be removed with the allowed modifications of the input parameters; e.g., variation of the fusion cross section within a 10% accuracy limit would be more than enough. We deliberately did not do it in order to avoid a pure parameter fitting which

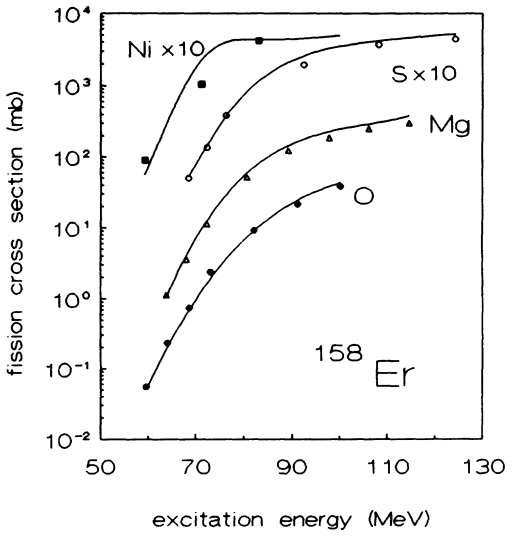

FIG. 2. Comparison of experimental data [3] with the results of our statistical-model calculations for fission of ^{158}Er obtained in ^{16}O+^{142}Nd, ^{24}Mg+^{134}Ba, ^{32}S+^{126}Te, and ^{64}Ni+^{94}Zr reactions.

could obscure the underlying physics. In any case it is clearly seen that using the best and an *a priori* fixed set of input parameters (allowing only for the variation of d) a very convincing reproduction of the experimental fission cross sections is achieved. This is in spite of the consistent inclusion of collective effects throughout the entire calculations, while in the original paper [3] it was argued that an incorporation of such effects would lead to the destruction of the general agreement between experimental data and statistical-model predictions. Analysis of Figs. 1 and 3 will help to solve these contradictions. First of all, in the energy range of our present interest, the rotational effects are not entirely damped at the yrast deformations and neither are they fully operative in the fission channel (see Fig. 1), as was supposed in Ref. [3]. The dependence of the fission cross section on the coupling between intrinsic and collective degrees of freedom can be qualitatively studied by multiplying $E_{\rm cor}$ in Eq. (12) with a constant χ and varying it between 0 and infinity. Setting $\chi=0$ corresponds to the complete damping of the rotational effects, leaving only intrinsic excitations (we may call it a spherical limit), while for χ equal to infinity we recover an adiabatic limit. All finite values of χ therefore correspond to the intermediate coupling of rotational and intrinsic motions. The effect of this coupling on the fission cross section is presented in Fig. 3. We note that, in the case considered, the fission cross section in the adiabatic limit is somewhat larger than the value obtained in the spherical limit. Roughly speaking, their ratio is approximately equal to the ratio of rotational enhancement factors for fission and particle emission channels, $(\mathcal{I}_\perp)_f t_f/(\mathcal{I}_\perp)_{\rm yr} t_{\rm yr}$. Even though the saddle-point moment of inertia is always larger, the final result may still depend on the most probable temperatures in the fission and particle emission channels. In very rare cases of excitations slightly above a high fission barrier (possible mostly at low spins), a larger temperature in the particle channels may win over the moment-of-inertia ratio, and the fission cross section in the adiabatic limit may become smaller than in the spherical limit. In any case, going back from the adiabatic toward the spherical limit, the fission cross section increases (see Fig. 3) because of the faster fadeout of the rotational enhancement factor in the particle channels (Fig. 1). The fission cross section reaches its maximum for χ around 0.2 and then falls down to the spherical limit. This maximum is, however, much lower than what one would expect if rotational enhancement were totally damped in the particle channels but still fully effective in the fission channel. This would lead to an increase of the fission probability by two orders of magnitude. If this does not happen, it is due to the rather slow energy and deformation dependence of our $Q_{\rm rot}$ function. Good agreement between experimental data and the results of our calculations confirms our choice of the damping function and of the physically motivated value for the χ parameter ($\chi=1$). In fact, we have performed calculations using different forms of the damping function [15], obtaining results which were visibly worse.

We also note a very weak dependence of the calculated fission cross section on the value of the level-density parameter a. Applying the standard relation $a=A/8$, which for ^{158}Er provides us with the value $a=19.8$, considerably higher than our value $a\simeq 15$, the fission cross section changes a few percent only, confirming that the results depend more on the ratio of the level densities in the fission and nucleon emission channels than on their absolute values.

Having convinced ourselves of the applicability of the model to the reactions studied, we may proceed to investigate the less apparent details of the reaction mechanism. First of all, we address the spin dependence of the fission probability (given by the ratio of the fission width

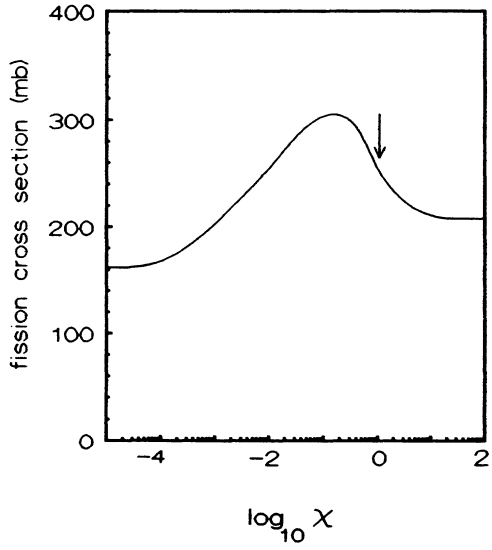

FIG. 3. Dependence of the fission cross section on the χ parameter (see text) in the case of the ^{32}S+^{126}Te incoming channel at an incident energy of 180 MeV. The arrow points to $\chi=1$, the value used in the calculation.

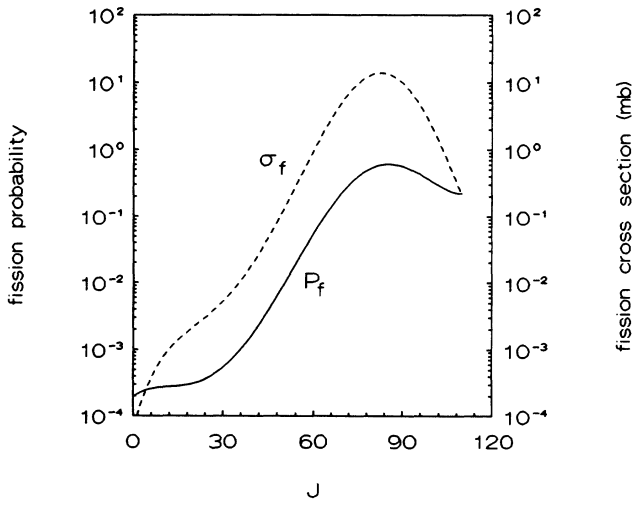

FIG. 4. Dependence of the fission probability (solid line) and the fission cross section (dashed line) on the compound-nucleus spin for the ^{32}S+^{126}Te incoming channel at an incident energy of 220 MeV.

to the total width, Γ_f/Γ_{tot}) as shown in Fig. 4. One observes a strong increase of the fission probability with increasing spin. There are two reasons contributing to this effect: (i) decreasing fission barrier and (ii) large moment of inertia of the saddle-point configuration, which makes the density of high-spin states in the fission channel much larger than the equivalent densities in the particle emission channels. It is worthwhile noting that since the CN population is also up to l_{fus}, an increasing function of the spin (due to the kinematical factor $2l+1$), an overwhelming contribution to the fission cross section comes from the very few spin values close to l_{fus} (see Fig. 4). A decrease of the fission cross section at the very last spin values is related to the vanishing population of these states in the projectile-target fusion. This observation is essential to our further discussion since all the effects we are going to discuss are a direct consequence of this particular spin dependence of the fission probability.

The most evident spin effect is a drastic growth of the fission cross section with increasing projectile mass for the fixed CN excitation energy (see Fig. 2). This finds a straightforward explanation in the fact that heavier projectiles bring about higher angular momenta, populating higher-spin states, which are of high fissility. It follows that the difference between the fission cross sections for two different incoming channels leading to the same CN excitation energy reflects the difference between maximal l values participating in the CN fusion (l_{fus}) in both cases. Obviously, this statement holds when the CN is the only mechanism contributing to fission.

Another spin effect brings us back to the determination of the input parameter d, which describes the fallout of the fusion cross section in the vicinity of l_{fus}. Figure 5 shows a typical dependence of the fission cross section in a function of d for two distinct CN excitation energies: the first one close to the fission threshold and the other one considerably higher. The fission cross section turns out to increase strongly with d in the first case, while for the higher energy this dependence practically disappears. The explanation is again given by the spin dependence of the fission probability. At low energies the CN states populated from the incoming channel lie in the spin region where the fission probability rapidly increases. Increasing d means shifting part of the fusion cross section toward higher spins, which have a higher fission probability, and thus the calculated fission cross section increases. For the higher-energy case, the same shift of the fusion

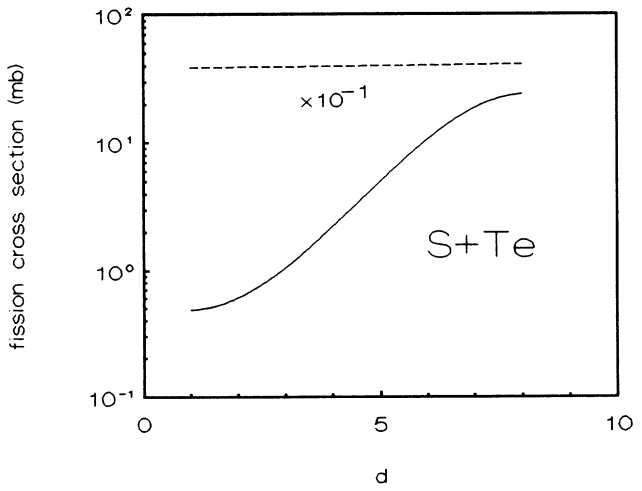

FIG. 5. Dependence of the fission cross section on the parameter d in the case of the $^{32}S+^{126}Te$ incoming channel at an incident energy of 150 MeV (solid line) and 220 MeV (dashed line).

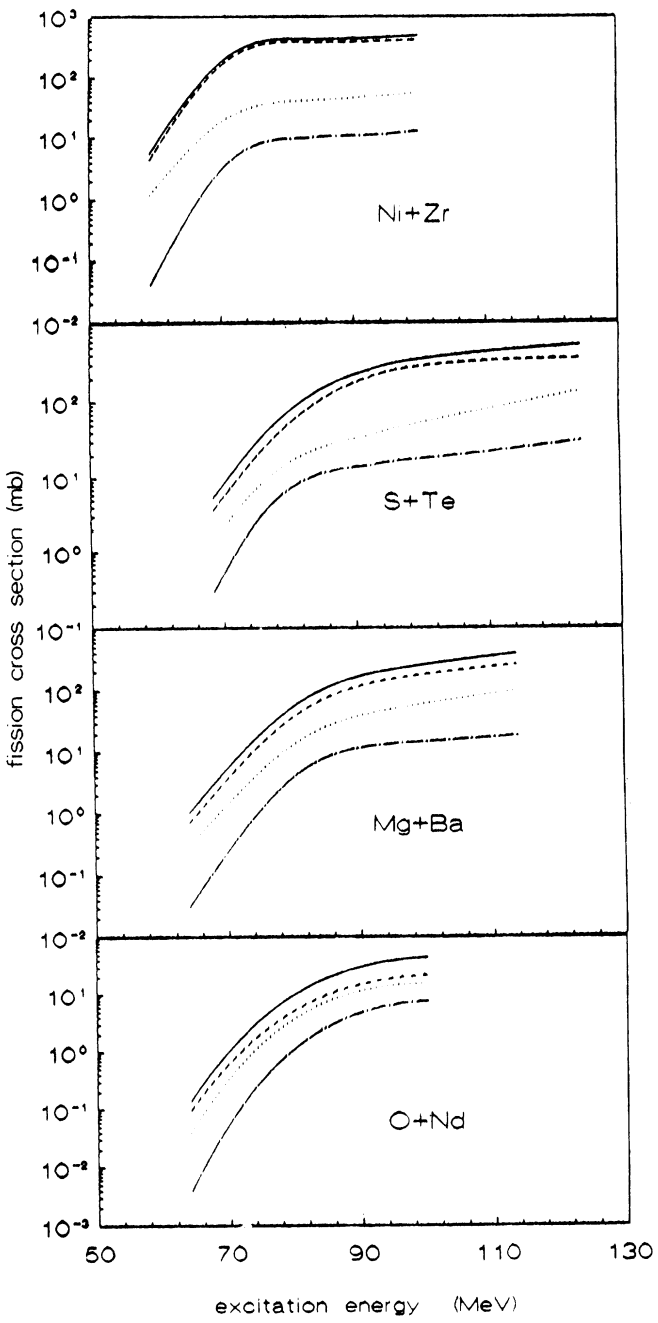

FIG. 6. Contributions of the multiple-chance fission cross sections to the total fission cross section (solid line) for the four different incoming channels considered. The dashed, dotted, and dot-dashed lines refer to first-, second-, and third-chance fissions respectively.

cross section does not make such a large difference since the fission probability tends to saturate approaching unity. This can be worded more generally by saying that the fission cross section is sensitive to the fusion spin distribution if l_{fus} is well below the l value, whereby the fission barrier vanishes. This fact makes *a priori* predictions of the fission cross sections right above the fission threshold difficult, but this may be turned to our advantage by using it for the determination of the CN spin distribution resulting from HI fusion, which is not a directly measurable quantity. Actually, in the present analysis, we obtained d equal to 1.5, 4.5, 4.5, and 1.0 for $^{16}O+^{142}Nd$, $^{24}Mg+^{134}Ba$, $^{32}S+^{126}Te$, and $^{64}Ni+^{94}Zr$ channels, respectively.

The third effect we are going to discuss is the relative probability of the multiple-chance fission for different projectile-target combinations. In Fig. 6 we decompose the results of our calculations, already presented in Fig. 2, into contributions coming from the fission of the initial CN (first-chance fission) and those which are due to the fission of the residual nuclei after emission of one and two neutrons (second- and third-chance fissions). Generally, one would expect that a multiple-chance fission can be characterized by the increasing shift in the excitation energy, which may approximately be related to the neutron binding plus average energy of the emitted neutron, i.e., the difference between excitation energy of the parent and daughter nuclei. Accordingly, the multiple-chance fission cross section should decrease with the number of neutrons emitted prior to fission and, in the first approximation, should depend on the neutron binding energies in the subsequent nuclei. In fact, such a general behavior is observed in Fig. 6. However, we would like to point out that in some cases the shapes of different multiple-chance fission cross sections are different, contradicting the assumption of the simple energy shift between subsequent fission chances. Moreover, for the $^{64}Ni+^{94}Zr$ channel, multiple-chance fission cross sections seem to differ by a factor other than a constant-energy shift. In Fig. 7 we plot percentage contributions of the first-, second-, and third-chance fissions to the total fission cross section for the four incoming channels leading to ^{158}Er at an excitation energy of 100 MeV. We chose this relatively high energy in order to have all three fission chances well established. By analyzing Fig. 7, we note that for the lightest projectile the first-, second-, and third-chance fissions contribute with 49%, 34%, and 17%, respectively. Considering heavier projectiles, the contribution of the first chance grows at the expense of the higher chances and for the $^{64}Ni+^{94}Zr$ system we find 85%, 12%, and 3%, respectively. Alternatively, the same effect may be worded in terms of the prefission neutron multiplicity, which turns out to decrease from 0.68 in the former case to 0.18 in the latter one. This may be understood as a depletion of the cross section available to fission resulting from the fission of the preceding nucleus in the chain. As we already know, this depletion increases with the projectile mass. This effect is enhanced by the fact that, because of the spin dependence of the fission probability, depletion mostly concerns the states of highest fissility. Neutron emission brings about a rather small change in angular momentum, and in any case, for highest-spin states, it tends to shift the population toward lower spins where more levels are available. Therefore neutron emission does not obscure fission depletion. If the fission probability of such states is high enough, the population of the high-spin states in the residual nucleus will be very low, leading to a considerable reduction of the next-chance fission.

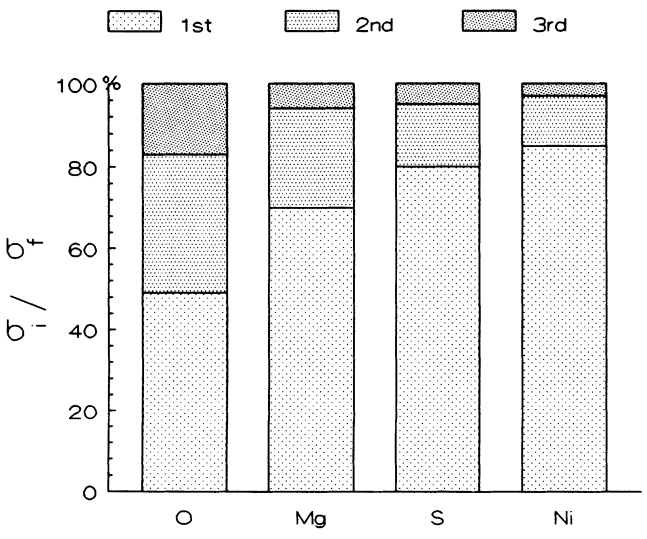

FIG. 7. Histogram of the relative contributions of the multiple-chance fission for the four incoming channels at the same excitation energy of 100 MeV.

V. SUMMARY

We have presented statistical-model calculations of the heavy-ion-induced fission cross sections using an *a priori* fixed set of input parameters and avoiding any numerical approximations. We have allowed for only one free parameter d, describing the angular momentum distribution of the fusion cross section, which in any case has only a marginal effect on the fission cross section at energies surpassing the fission threshold by more than few tens of MeV. In principle, there are no grounds to expect d to be independent from energy, but its relatively small influence on the fission cross section at higher energies does not allow a trustworthy determination of its energy dependence. However, at the energies right above the fission threshold, a large sensitivity of the fission cross section to the value of the parameter d may be used to determine the fusion spin distribution. We obtain a very good description of the experimental data, allowing for the nonadiabatic coupling of the collective and intrinsic degrees of freedom in the level densities. This contrasts with the results of Ref. [3], where it was claimed that inclusion of such effects would destroy the agreement. By analyzing the answer of the calculated fission cross section to the gradual transition from the case with no collective effects to the adiabatic limit (collective effects included without any damping), we have found that the fission cross section is only slightly different between these two limits (being larger in the adiabatic limit),

reaching its maximum in between. This behavior could be used to discern damping of the collective effects, especially in the high-energy range where the fusion spin distribution parameter d does not affect the results. In this work we have found that the physically motivated assumption that the collective effects fade out to $\frac{1}{2}$ at a temperature equal to the Coriolis energy is consistent with the experimental data, and therefore we do not consider this issue as a degree of freedom in the calculations. Accordingly, at higher energies there are essentially no possibilities of changing the results of our calculations.

Our code is capable of an approximate treatment of viscosity effects, but agreement obtained without these effects did not call for their inclusion. In fact, the use of a reasonable value (about 0.8×10^{21} s^{-1}) for the viscosity parameter would lead to a decrease of the calculated fission cross sections by 10–20 %, leaving the agreement with the experimental data essentially unchanged. Moreover, the same changes can be obtained by the modification of the coupling between collective and intrinsic degrees of freedom (i.e., damping of collective effects). For these reasons we have decided to neglect the viscosity effects in order to avoid the introduction of a free parameter. This does not mean that the dissipation effects are totally negligible, but it certainly indicates that the phase-space arguments prevail by far in the considered energy range.

The most striking feature of the heavy-ion-induced fission is a strong increase of the fission probability with CN spin. A direct consequence of this effect is a strong correlation between the fission and fusion cross sections, which may be used to determine the latter once the former is known experimentally.

ACKNOWLEDGMENTS

This work was supported by the Istituto Nazionale di Fisica Nucleare, Ministero dell'Universita e della Ricerca Scientifica e Tecnologica. We wish to thank Dr. L. Hobbins for useful suggestions during the revision of the English text. We also acknowledge A. Sierk for making routine BARMOM available.

[1] M. Herman, A. Marcinkowski, and K. Stankiewicz, Comput. Phys. Commun. **33**, 373 (1984).
[2] S. E. Vigdor and H. J. Karwowski, Phys. Rev. C **26**, 1068 (1982).
[3] J. van der Plicht, H. C. Britt, M. M. Fowler, Z. Fraenkel, A. Gavron, J. B. Wilhelmy, F. Plasil, T. C. Awes, and G. R. Young, Phys. Rev. C **28**, 2022 (1983).
[4] D. L. Hill and J. A. Wheeler, Phys. Rev. **89**, 1102 (1953).
[5] R. Bass, Phys. Rev. Lett. **39**, 265 (1977).
[6] A. Bohr and B. R. Mottelson, *Nuclear Structure* (Benjamin, New York, 1975), Vols. I and II.
[7] A. V. Ignatyuk, K. K. Istekov, and G. N. Smirenkin, Yad. Fiz. **29**, 875 (1979) [Sov. J. Nucl. Phys. **29**, 450 (1979)].
[8] F. D. Becchetti and G. W. Greenlees, Phys. Rev. **182**, 1190 (1969).
[9] A. D'Arrigo, G. Giardina, and A. Taccone, Phys. Lett. B **262**, 1 (1991).
[10] C. J. Bishop, I. Halpern, R. W. Shaw, Jr., and R. Vandenbosh, Nucl. Phys. **A198**, 161 (1972).
[11] BARMOM, No. 9677, National Energy Software Center, Argonne National Laboratory, Argonne, IL 60439.
[12] G. Andersson, S. E. Larsson, G. Leander, P. Möller, S. G. Nilsson, I. Ragnarsson, S. Åberg, R. Bengtsson, J. Dudek, B. Nerlo-Pomorska, K. Pomorski, and Z. Szymański, Nucl. Phys. **A268**, 205 (1976).
[13] A. H. Wapstra, G. Audi, and R. Hoekstra, At. Data Nucl. Data Tables **39**, 281 (1988).
[14] C. M. Lederer and V. S. Shirley, *Tables of Isotopes*, 7th ed. (Wiley, New York, 1978).
[15] E. M. Rastopchin, Yu. B. Ostapenko, M. I. Svirin, and G. N. Smirenkin, Yad. Fiz. **49**, 24 (1989) [Sov. J. Nucl. Phys. **49**, 15 (1989)].

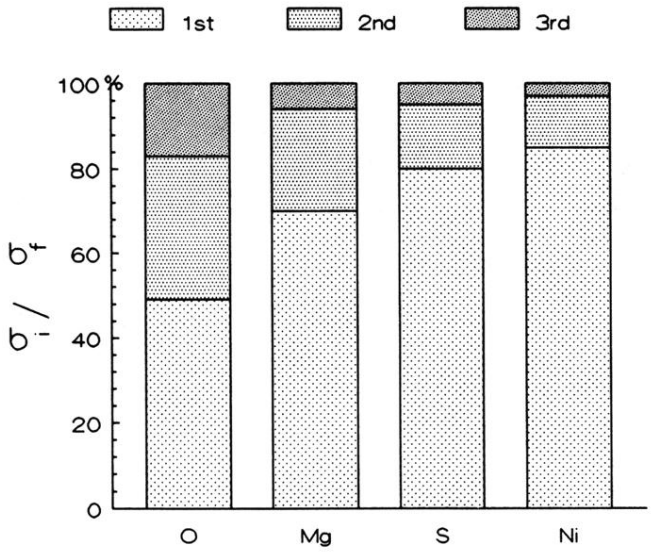

FIG. 7. Histogram of the relative contributions of the multiple-chance fission for the four incoming channels at the same excitation energy of 100 MeV.